Landslides (2012) 9:117–130
DOI 10.1007/s10346-011-0277-5
Received: 20 May 2010
Accepted: 30 May 2011
Published online: 11 June 2011

Guo-Quan Wang

Kinematics of the Cerca del Cielo, Puerto Rico landslide derived from GPS observations

Abstract Global positioning system (GPS) technologies have been increasingly employed to monitor landslide movements. This paper demonstrates the use of GPS in the study of a creeping landslide in Ponce, Puerto Rico. The landslide is primarily composed of chalk colluvium that extends to depths of about 30 m at the head zone and 2 to 3 m at the toe zone. The slip surface lies at the base of the chalk colluvium, which slides southeast over a weathered brown mudstone unit. GPS monitoring of the landslide began in March 2008. Both campaign rapid static and continuous static GPS surveying methods were applied. Precision at the level of 0.5 mm horizontally and 1.3 mm vertically was achieved through 24-h continuous GPS monitoring. Rainfall data from a local weather station was also integrated into the study. Rainfall heavily influenced the movements of the landslide. A heavy rainfall in September 2008, which dumped 50 cm rain on the landslide area over a 4-day period, temporarily accelerated the sliding and generated rapid movement of 1m horizontally and 0.5 m vertically. The slide slowed markedly after this significant movement. A prolonged moderate rainfall in November 2009 also temporarily accelerated the sliding. The landslide remains active. The creeping appears likely to continue in the future with short bursts of rainfall-induced rapid movements. Potential landslide causes are investigated, and two measures to minimize future risk are proposed at the end of the article.

Keywords Landslide · Puerto Rico · GPS · Rainfall

Introduction

Puerto Rico is located in the northeastern Caribbean Sea, east of the Dominican Republic and west of the Virgin Islands. Mountainous terrain and tropical climate combine to make the island one of the most landslide-prone areas in the USA (Jibson 1986). Much of Puerto Rico is characterized as being moderately to highly susceptible to landsliding (Monroe 1979). One of the most important and catastrophic landslides occurred in Mameyes, Ponce in October 1985 (Silva-Tulla 1986). The death toll at Mameyes, totaling over 100 people, made it the worst loss of life from a single landslide in US history (Jibson 1986). The Cerca del Cielo, Ponce landslide studied in this article is only about 5 km away from the Mameyes landslide site. Both landslides lie on the same geological unit, the Juana Diaz Formation, a typically troublesome geologic unit because of its rich plastic clay size particle content. The Ponce area has suffered significant losses from landslides in the past. According to a US Geological Survey (USGS) investigation, 34% of the municipality Ponce is highly susceptible to rainfall-triggered landsliding, 24% is moderately susceptible, and only 9% is less than moderately susceptible (Larsen et al. 2004).

Rolling hills dominate the topography of the area, with most relatively flat lots being the result of cut-to-fill operations. Figure 1 shows an aerial view of the Cerca del Cielo community. The community is home to about 70 families. The oldest houses in the urbanization are about 40 years old and are located on the western side of the main entrance road. Communication with local residents has indicated that the houses on the west side of the entrance road are on cut lots, while the residences on the east side of the entrance road are mostly on filled lots. Investigation by a local geotechnical engineering company showed the existence of heterogeneous and organic-rich materials inside the filled area, suggesting poor quality control during the fill works (Suelos Inc. 2008). The landslide has cut the sole access road to the whole community and destroyed ten houses on the sliding mass (Fig. 2). Another 15 houses close to the sliding mass have been abandoned. The creeping mass covers the entrance area of the community and affects the entire community as it involves the only access road as well as utility lines (water, power). The community was without running water for several months during late 2008 and early 2009 due to severe damage to the water pipes.

Continuous monitoring is essential to studying the kinematics and to predicting the behavior of landslides. Measuring superficial displacements is the simplest way to observe the evolution of a landslide and to analyze the kinematics of the movement. In the last decade, global positioning system (GPS) techniques have been widely applied to monitor superficial displacements in unstable areas, both as a complement to conventional surveying methods and as an alternative to them (Gili et al. 2000; Malet et al. 2002; Coe et al. 2003; Sato et al. 2003; Squarzoni et al. 2005; Bruckl et al. 2006; Tagliavini et al. 2007; Psimoulis et al. 2007; Peyret et al. 2008; Wang et al. 2011). These studies confirmed the GPS survey technique as a very useful tool in landslide monitoring. In general, GPS technologies increase accuracy, productivity, monitoring capability, rapidity, flexibility, and economy as compared to classical geodetic survey techniques. This study used campaign rapid static and continuous static GPS surveying methods to monitor an active landslide. Both static and rapid static GPS methods involve using two GPS receivers to simultaneously measure a baseline vector. The static survey requires a long observation time from a few hours to a day. The rapid static survey is essentially the same as the static GPS surveying method, except that observation can be carried out in a time period as short as a few minutes. The rapid static method was developed from the classical static GPS method, with improved algorithms that speed the procedure (Frei and Beutler 1990). Landslide displacements in this study are described by the changes in the baseline length between a reference GPS antenna and a rover GPS antenna in north–south (NS), east–west (EW), and vertical directions. Both L1 and L2 observations were used to form a double difference by differencing the between-station differences and between-satellite differences. The major aims of the study are (a) to quantify the spatial and temporal evolution of the landslide, (b) to study the influence of rainfall on landslide activity, and (c) to investigate the reasons behind the landslide failure and propose solutions to minimize future damage and potential risk.

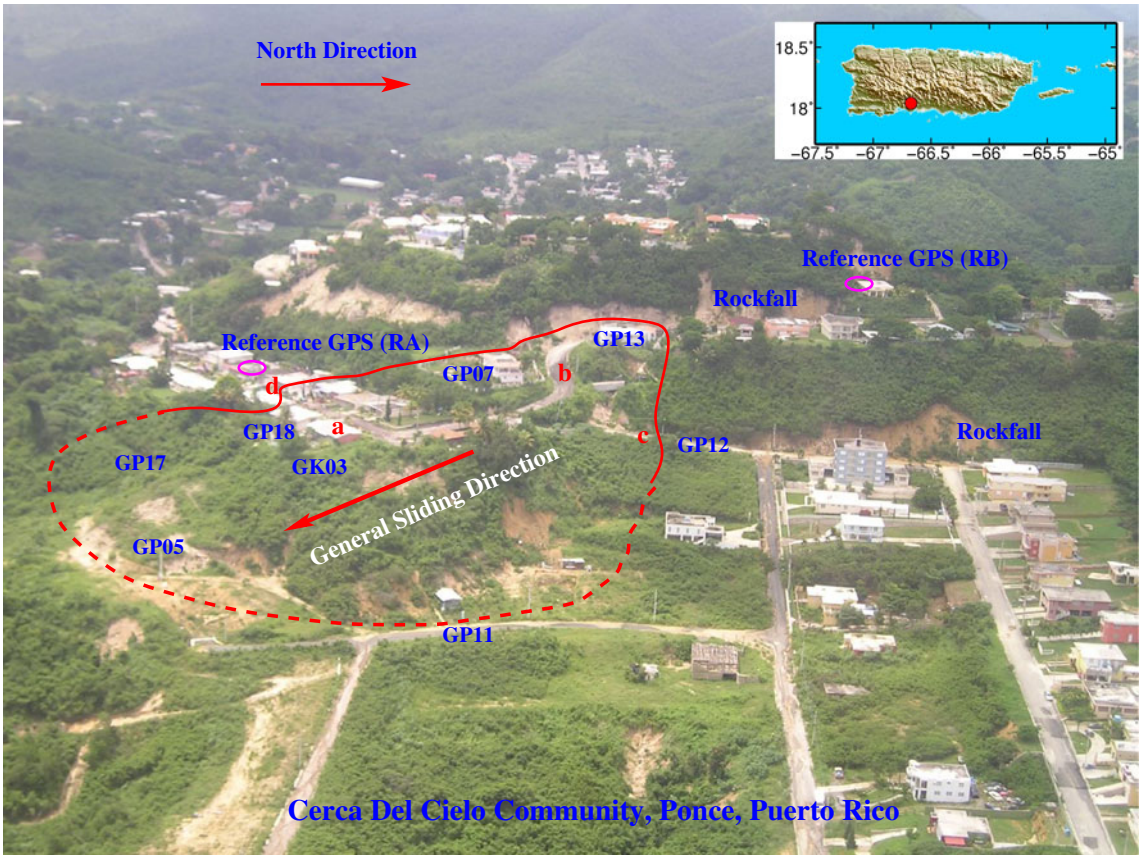

Fig. 1 An aerial view of the Cerca del Cielo community and the landslide (photo: James Joyce, September 2008). The *solid line* indicates scarps and cracks that can be identified in the field. The *dashed line* indicates the boundaries constrained by the GPS measurements and field investigations. The *red arrow* indicates the general sliding direction of the sliding mass

Geological setting

The USGS geological map of the Penuelas and Punta Cucharra Quadrangles (Krushensky and Monroe 1978) shows the Cerca del Cielo community as underlaid by the Chalk Member and the Mudstone Member of the Juana Diaz Formation of Oligocene and Miocene age. The landslide formed at the base of a 50-m-high steep cliff composed of the Chalk Member of the Juana Diaz Formation. Blocks and pieces of the Chalk Member comprised the

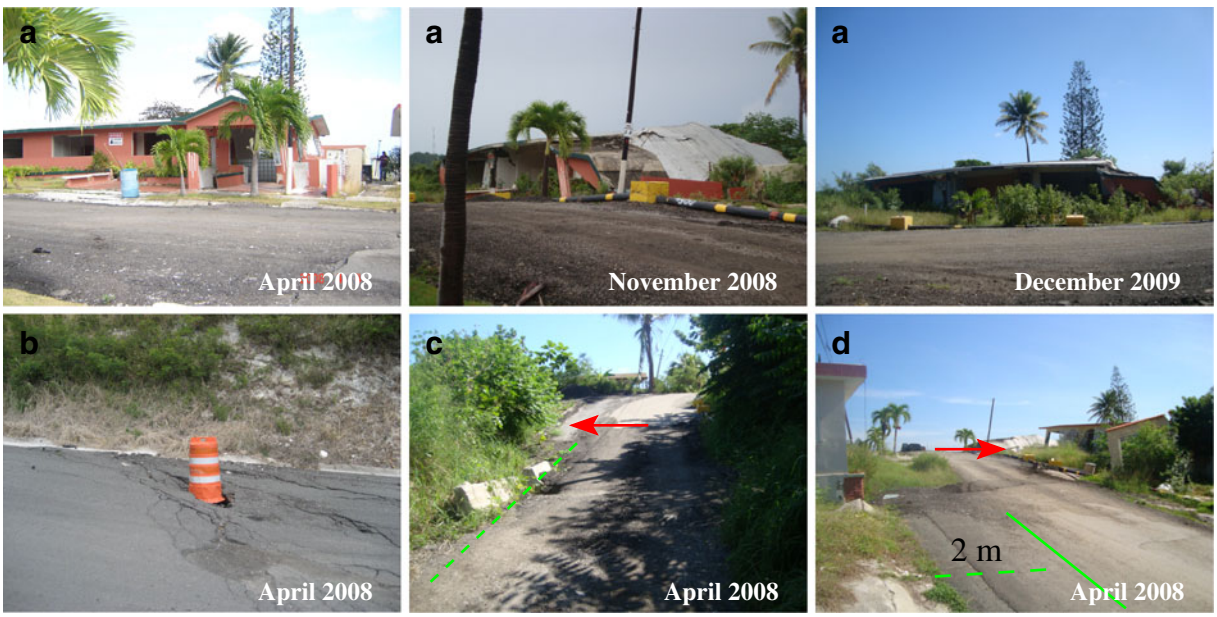

Fig. 2 Buildings and roads destroyed by the continuous movement of the landslide. Photo locations are marked in Fig. 1

Quaternary colluvial (or landslide) deposits along the base of the cliff faces. Some exposures of the chalk colluvium exhibit stratification, channels, and fossilized land snails, which indicate that the colluvium was formed through a series of depositional events rather than a single landslide event. Geologic and geotechnical data as well as field observations at the site indicate that the present landslide is a reactivated ancient landslide mass (Joyce 2008).

The sliding mass is approximately 300 m long from head to toe. The landslide head is approximately 30 m wide extending to 150 m near the toe. According to local borehole information, the chalk colluvium extends to depths of about 30 m at the head zone and 2 to 3 m at the toe zone. The toe zone consists of highly disrupted colluvium materials and building debris. The total area of the sliding mass is about 30,000 m^2. The landslide features a main scarp as high as 3 m at the head area (Fig. 3). The head scarp is very steep, indicating that the sliding materials (chalk colluvium) are strong. Standard penetration tests performed in the colluvium area showed *N* values of up to 28 blows per foot (Suelos Inc. 2008), which also indicates that the colluvium materials are very stiff as well as strong. The potential weak link would be at the bottom of the colluvium. Inclinometer, borehole, and slip striation data further confirmed that the sliding plane lies at the base of the chalk colluvium, which overlies the weathered Mudstone Member of the Juana Diaz Formation. The chalk colluvium is sliding as a block over the weathered mudstone. The sliding plane inclines about 50° at the head, 15° near the center, and is nearly horizontal at the foot of the sliding mass (Joyce 2008).

A well-developed paleosol horizon separates the colluvium and weathered Mudstone Member. The paleosol and weathered mudstone suggest that the mudstone underwent a long period of exposure prior to being covered by the chalk colluvium. Long-term weathering and erosion of the mudstone obliterated most of the primary structure and reconstituted the mineralogy into plastic clay. The plastic clay layer is strong when dry but becomes much weaker when wet. There are rich plastic clay materials in the weathered Mudstone member of the Juana Diaz Formation, which cause low inherent strength and slope stability problems in many areas of Ponce.

Campaign GPS monitoring

The movement of the landslide was initially identified in the summer of 2007. A campaign GPS surveying network consisting of one reference benchmark (RA in Fig. 1) and 25 benchmarks spreading both inside and outside of the sliding mass was put in place in March 2008 (Fig. 4). The reference benchmark was on the roof of a one-story building. The building lay about 30 m from the nearest landslide scarp. The baseline lengths of the campaign GPS measurements were less than 400 m. The equipment used as the reference GPS was a Trimble Zephyr Antenna with a NetRS receiver. Two Topcon GB-1000 campaign GPS units were used for the rovers. Two 2-m fixed bipods were used to mount the GPS antennas at the rover points. The campaign surveying was performed, on average once every 2 weeks, during the period from March 2008 to March 2009. The observation time at each rover benchmark was 20 min. The sampling interval of raw GPS data was 5 s. The cut off angle degree was set at 15°. There were normally eight to ten satellites available at the landslide site. The commercial software Topcon Tools (Version 7.2) developed by Topcon Inc. (http://www.topconpositioning.com) was applied to process the rapid static data. The initial campaign survey took place on March 21, 2008. The baselines from the initial campaign were set as zero measurements. The displacements obtained from all subsequent campaigns were referred to the zero measurements. The stability of the reference station was further evaluated by studying the baseline length between the reference station and a nearby permanent GPS station (P780, 6 km away) operated by the Plate Boundary Observatory GPS Network (http://www.earthscope.org). Neither measurable movements nor visible cracks were identified on the reference building during the 1-year campaign surveying period.

It is widely recognized that baseline length and observation time play major roles in the accuracy of GPS surveying. According to the Reference Manual of Topcon Tools (2007) and previous empirical studies (e.g. Eckl et al. 2001; Soler et al. 2006; Dogan 2007), rapid static surveying with such a short baseline (<400 m) could attain sub-centimeter accuracy in horizontal directions. Taking into consideration the inaccuracy associated with bipod setups and the inconsistencies of antennas in the field, accuracy on the order of 2 cm horizontally and 5 cm vertically was expected for the campaign surveys conducted in this study.

The boundaries of the landslide

The head scarp and western margins of the landslide could be visually identified in the field, but the eastern and southern side margins were not obvious when the GPS monitoring began. The blue lines shown in Fig. 4 indicate the boundaries of the active sliding mass. The solid line indicates clear scarps which can be observed in the field. The dashed line indicates estimated margins along the western flank and the toe area, constrained by GPS measurements and field investigations. Measurements at benchmarks outside the boundary did not show measurable movement during the period from March 2008 to March 2009. The suspected active landslide area drawn out by a local geotechnical engineering company was about 50 m east of benchmark GP11 (Suelos Inc. 2008), while GPS measurements taken from this study did not show measurable movement at benchmark GP11. Accordingly, the previously suspected active area was constrained to the west side of GP11. Measurements at GP05 and GP17 showed continuous rising, which identified the frontier of the landslide toe zone.

Landsliding vs. rainfall (March–December 2008)

Figure 5 illustrates the correlation between local rainfall and the landslide movements measured at four benchmarks (GP07, GP13, GP03, and GP18) from March to December 2008. GP07 and GP13 were located at the head of the landslide; GK03 and GP18 were located at the upper edge of the foot slope. The top plot illustrates accumulated rainfall recorded in the vicinity of the landslide area by a USGS weather station, about 5 km northwest of the landslide site. The bottom plots show landslide movements. There was a significant rapid slide during September 2008, which coincided with an extraordinarily heavy rainfall produced by a tropical storm passing over Puerto Rico from September 20 to 23, 2008. This storm produced torrential rainfall over Puerto Rico and resulted in six fatalities and $48 million in damages (Banuchi 2008). The storm strengthened to a hurricane on September 27

Fig. 3 Photos showing the head scarp (left) and the toe are (right) of the landslide

(category I) and was named Kyle (Avila 2008). The total rainfall in the landslide area during the 4-day period of September 20 to 23 amounted to 50 cm. The total landslide movement during and shortly after the storm was about 1 m horizontally and 0.5 m vertically. Many of the benchmark sites were inaccessible after the storm. The average sliding rates at the head were 6 cm/month horizontally and 2.5 cm/month vertically before the storm and 1 cm/month horizontally and 0.7 cm/month vertically after the storm. The downgrade of the creeping rates may have been a result of a shift of the center of the whole sliding mass from a higher attitude to a lower attitude. The head zone subsided nearly 2 m, while the toe zone rose about a half meter during September and October, 2008. The driving force was reduced and the resistance force was increased. As a result, the creeping of the sliding mass slowed after the significant slide.

The right-hand column of Fig. 5 is a subset window (15 days) showing the close relationship between the heavy rainfall and rapid landslide movements. The campaign GPS measurements on September 19, 2008 (before the storm) and September 28, 2008 (shortly after the storm) identified total movement as 1 m horizontally and 0.5 m vertically at the head zone during the 10-day window. The landslide cut through a road at the head zone (see Figs. 1 and 4). The head may have channeled large amounts of runoff water into the sliding mass, through the head scarp, and have accelerated the sliding. Many local residents witnessed the significant sliding during, and shortly after, the storm. One resident said they had to cut the scarp (caused by subsidence) and fill the gap (caused by horizontal movement) across the road in the head area in order to allow cars to drive through safely during the storm.

Heavy rainfall has been recognized as one of the major triggers of catastrophic landslides all over the world (Jibson 1986; Larsen and Simon 1993; Baum et al. 1998; Mora et al. 2003; Guzzetti et al. 2008; Larsen 2008). Rain water infiltrates into the ground and fills the void spaces among soil particles and rock fissures. The water pressure rises when the amount of water infiltrating into the ground increases.

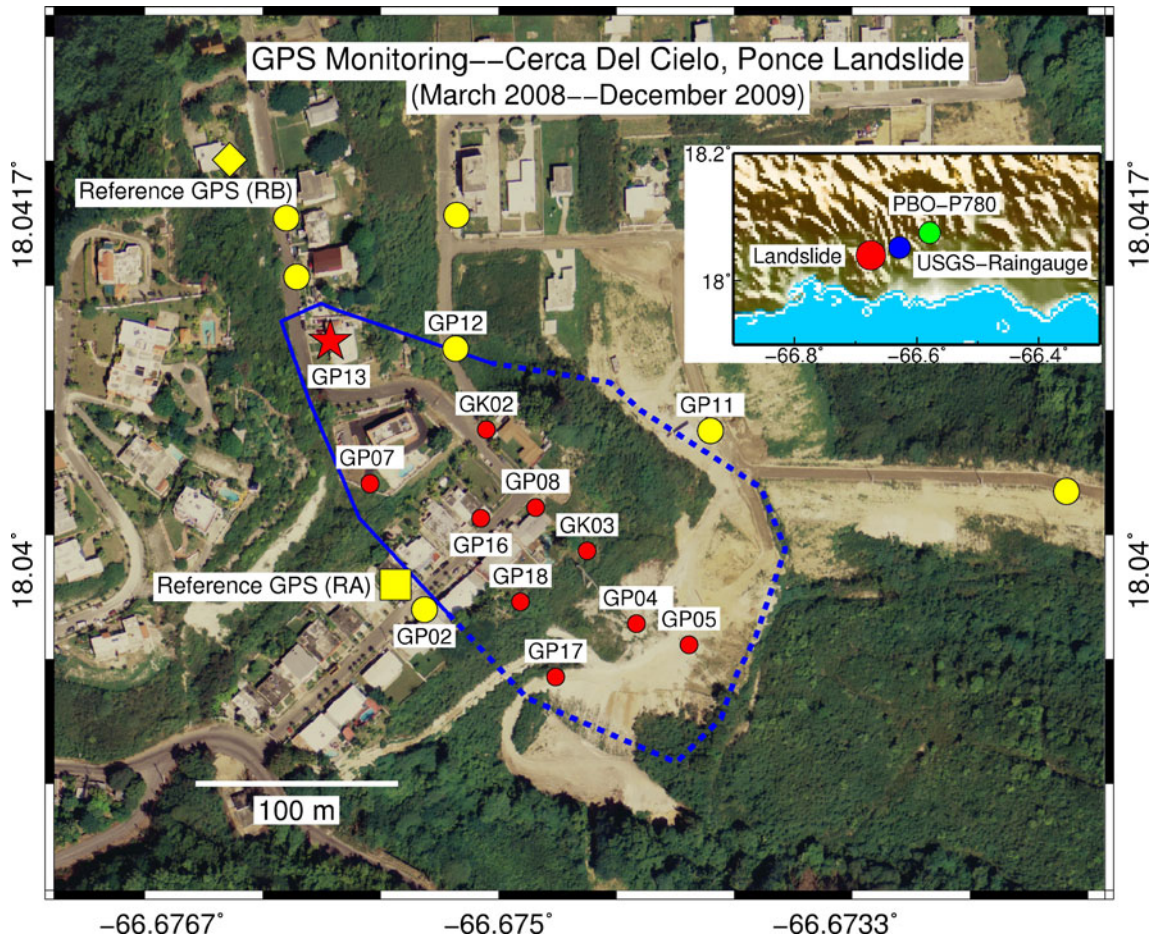

Fig. 4 Map showing locations and names of benchmarks installed for the campaign GPS surveying. The campaign surveying network included one reference (RA) and 25 rover benchmarks. A few benchmarks were outside of this map. The *solid and dashed lines* indicate the margins of the sliding mass. All benchmarks outside the sliding mass did not show measurable movements during the period from March 2008 to December 2009

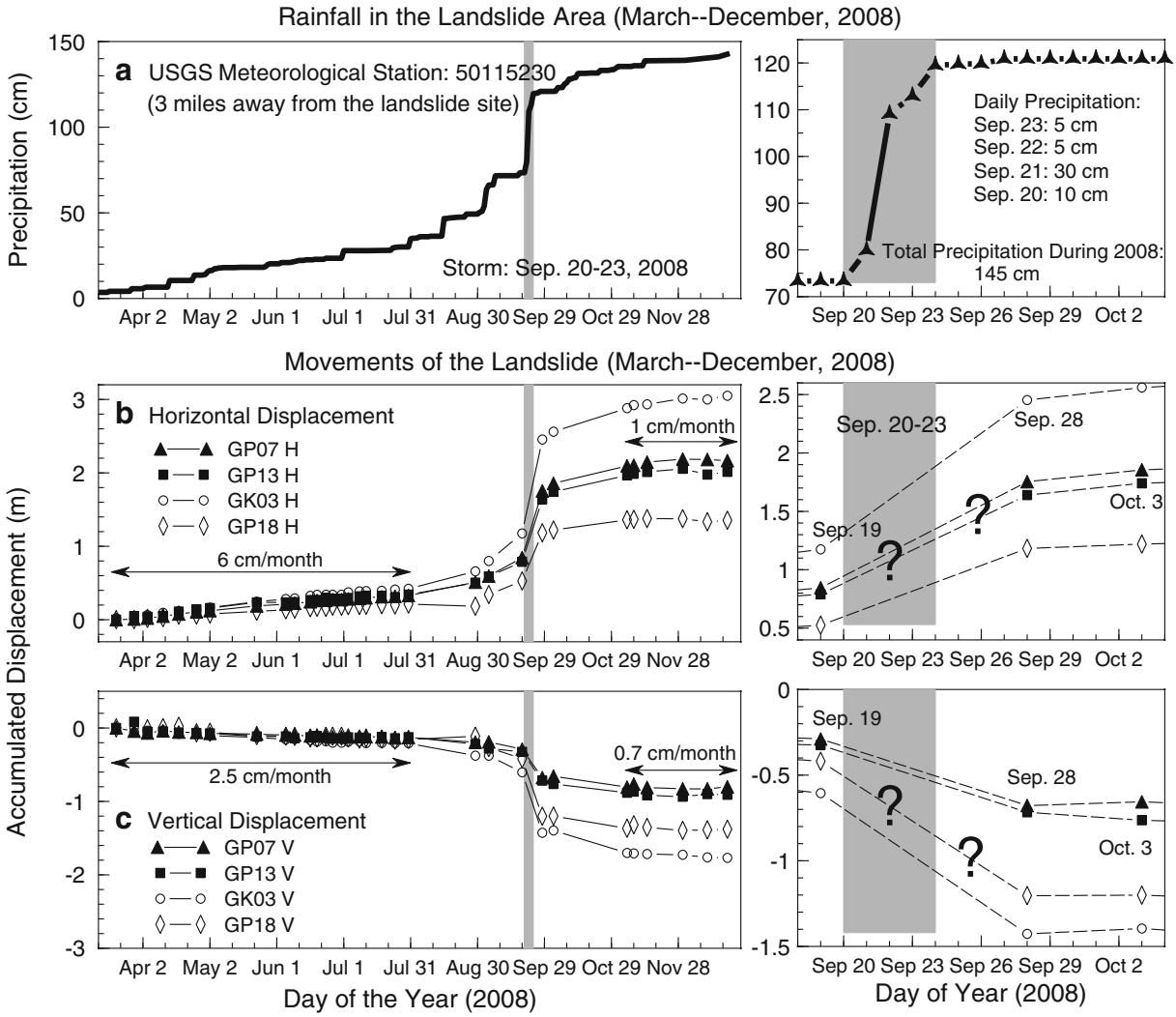

Fig. 5 Plots showing strong correlation between rainfall and landslide movement from March to December 2008. The *top row* shows the accumulated rainfall recorded at a nearby USGS Meteorological Station, about 5 km northeast of the landslide site (Fig. 4). The *middle and bottom rows* illustrate the GPS-measured horizontal and vertical movement at four benchmarks. GP03 and GP17 were at the head zone; GK03 and GP18 were at the middle of the landslide. The *right-hand column* is a 15-day window showing the landslide movement during, and shortly after, the heavy rainfall of September 20 to 23, 2008

A rise in pore water pressure causes a drop in effective stress, thus reducing the shear strength of the soil. A rapid slide occurs when the shear stress exceeds the shear resistance of the geologic materials. A rainfall threshold published by Larsen and Simon (1993) provides a preliminary method for estimating the accumulation and duration of rainfall likely to trigger landslides in the central mountain area of Puerto Rico. According to the experienced method, the number of rainfall-triggered landslides will increase substantially with a rainfall accumulation of up to 20 cm or more during a 24-h period. The rainfall amounts recorded by the local USGS weather station (see Fig. 4) were 10, 30, 5, and 5 cm during September 20, 21, 22, and 23, 2008, respectively. The rainfall on September 21 was enough to trigger landslides in the area. The storm triggered many landslides and floods in Ponce and other areas of Puerto Rico. Landslides and flooding are often closely associated.

Displacement vectors

Figure 6 illustrates horizontal and vertical displacement vectors measured at benchmarks within the sliding mass during August, September, and October 2008, respectively. Note that benchmarks outside the sliding mass did not show measurable movements. The maximum monthly movements during August, September, and October 2008 were 25, 180, and 42 cm horizontally and 17, 105, and 27 cm vertically, respectively. The significant movements during September correlated to the heavy rainfall shown in Fig. 5. The size and direction of the sliding vector varied slightly at different benchmarks. The sliding mass generally moved in a southeastern direction (about SE45°), with the exception of the toe benchmark (GP17), which slid to the southwest. Measurements at benchmarks indicated subsidence, with the exception of two toe benchmarks (GP05 and GP17), which continuously rose during the campaign surveying period.

Figure 7 illustrates the horizontal displacement vectors at the two head benchmarks (GP07 and GP13) and two toe benchmarks (GP05 and GP17) during a longer time span, from March 2008 to December 2009. The sliding directions at head sites GP07 and GP13 were SE33° and 49°, respectively. The sliding directions were considerably constant throughout the time range. The sliding

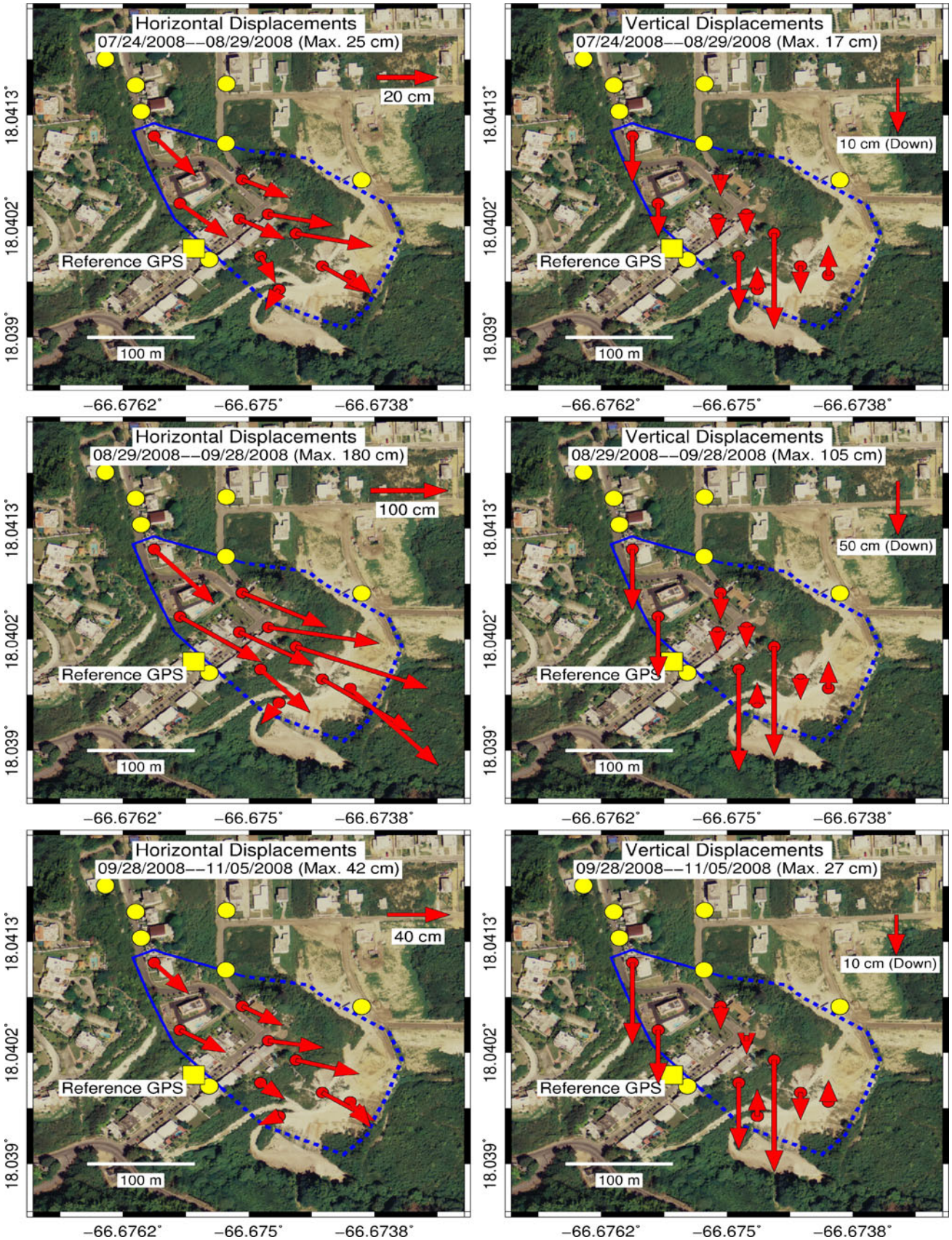

Fig. 6 Plots showing horizontal and vertical sliding vectors measured at benchmarks during August, September, and October of 2008. The large displacements in September were mostly caused by the heavy rainfall of September 20 to 23, 2008. The names of these benchmarks are marked in Fig. 4

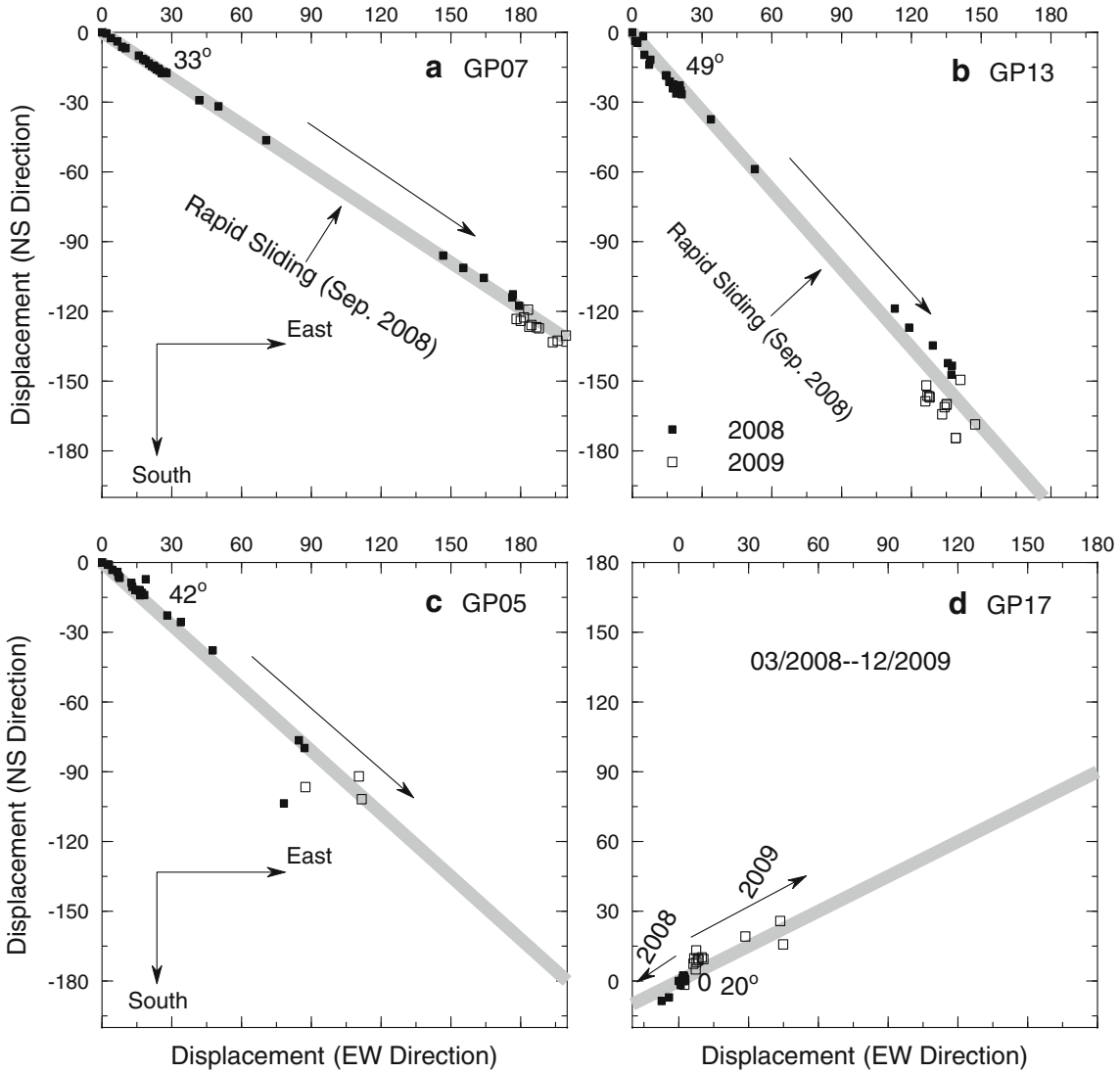

Fig. 7 Plots showing benchmark sliding tracks on the horizontal plane during the time span of March 2008 to December 2009. Benchmarks GP07 and GP13 were at the head area; GP05 and GP17 were at the toe area

direction at toe site GP05 was SE42°, which also remained constant during the time period, while the direction at toe site GP17 changed by 180° at the beginning of 2009. The benchmark GP17 was pushed about 20 cm to the south west due to the rapid horizontal extension of the toe zone during the storm in September 2008 (Fig. 6). The benchmark was then dragged to the northeast after the storm. This point moved about 30 cm northeast during 2009.

Changing of the landslide size

The sliding mass showed well-defined zones of depletion and accumulation. The depletion zone (the head area) was characterized by minor scarps and several traverse cracks. The accumulation zone (the toe area) was characterized by horizontal spreading and vertical rising. Kinematic heterogeneities in the landslide body were recognized by displacement vectors illustrated in Fig. 6. Figure 8 illustrates the changes in benchmark-to-benchmark distances between one head benchmark (GP13) and two toe benchmarks (GP05 and GP17) during the time span of March 2008 to December 2009. The distances between the head benchmark GP13 and the two toe benchmarks GP17 and GP05 were reduced by 2 and 0.7 m horizontally and 1.3 and 1 m vertically, which indicated shrinking of the landslide in the sliding direction. The distance between the two toe benchmarks, GP05 and GP17, increased by 0.8 m horizontally and 0.3 m vertically during the time span, which indicated extension of the toe area.

Continuous GPS monitoring

Campaign measurements of superficial displacements across the landslide mass showed significant effects of rainfall on the landslide and promoted concerns about potential catastrophic failure of the whole sliding mass during future heavy rainfalls. The sliding mass lies on a dip slope. The toe area is quite flat and open, providing enough space for further development in the future. Rainfall precipitation is one of the most important factors contributing to landsliding in Puerto Rico (Monroe 1964, 1979; Jibson 1989; Larsen and Simon 1993; Larsen and Torres-Sanchez 1996, 1998; Wang et al. 2011). August to October is the typical

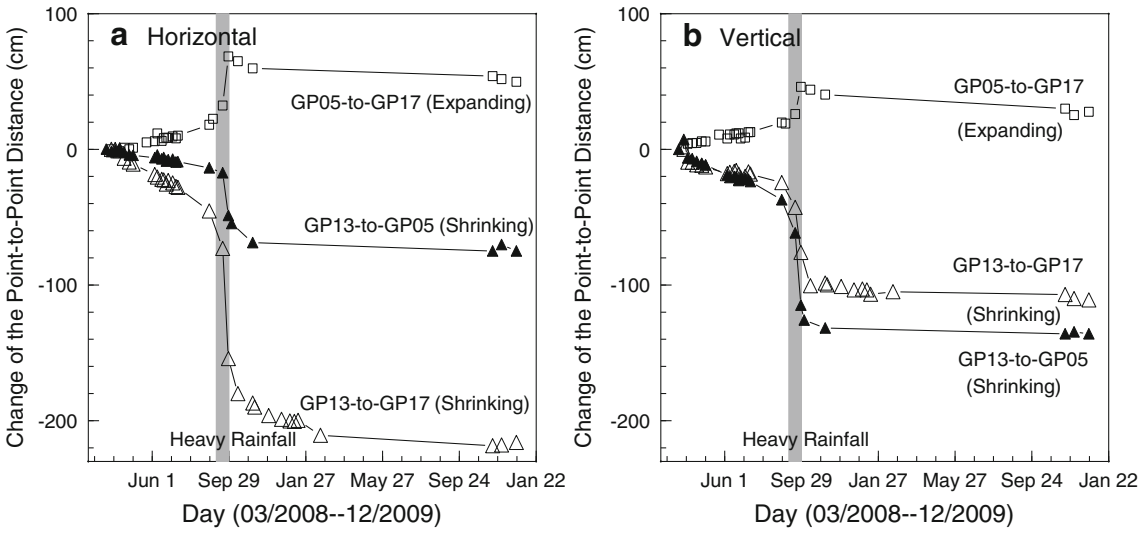

Fig. 8 Plots showing the changes in the size of the sliding mass during the time span of March 2008 to December 2009. The distances between head benchmark GPS13 and two toe benchmarks GP05 and GP17 were increased, while the distances between the two toe benchmarks were decreased

storm season for Puerto Rico. Most catastrophic landslides occur during this season, such as the October 7, 1985 Mameyes, Ponce landslide. The Mameyes landslide occurred following 2 days of a heavy rainfall. The campaign GPS surveys during 2008 further confirmed the significant effects of heavy rainfall on landslide movements. In order to further study the close relationship between rainfall and the landslide movement, a rain gauge and a continuous GPS monitoring system were equipped at the head of the landslide prior to the storm season of 2009 (Fig. 9). The system included a rover station installed on the roof of a two-story building and a reference station (RB in Fig. 1) outside the sliding mass. The distance between the reference and rover stations was 130 m. Both the reference and rover GPS stations were equipped with Trimble NetRS receivers and choke ring antennas (model TRM49700.00; Fig. 10). The receivers were configured to simultaneously record 15-s-per-sample, 1-sample-per-s, and 10-sample-per-s GPS data. Only the 15-s-per-sample data were used in this study. The rain gauge was installed at the reference GPS site, and the precipitation data were read daily by the owner of the reference building.

Daily resolution

The GAMIT GPS software developed at MIT (Herring et al. 2009) was used to process 24-h continuous data for this study. The Topcon software was not efficient for handling 24-h sessions. Figure 11 illustrates the daily displacement time series (NS, EW, and vertical) of the landslide recorded by the continuous GPS from June 1 to December 31, 2009. Each point represents the average position during a day-long period (24 h). The top row illustrates the accumulated rainfall recorded by the local rain gauge. The displacement time series show steady movement during the seven months with the exception of a rapid slide in the middle of November 2009. The total movement during these 7 months was 4, 5, and 3 cm in NS, EW, and vertical directions, respectively. The displacement time series in three directions

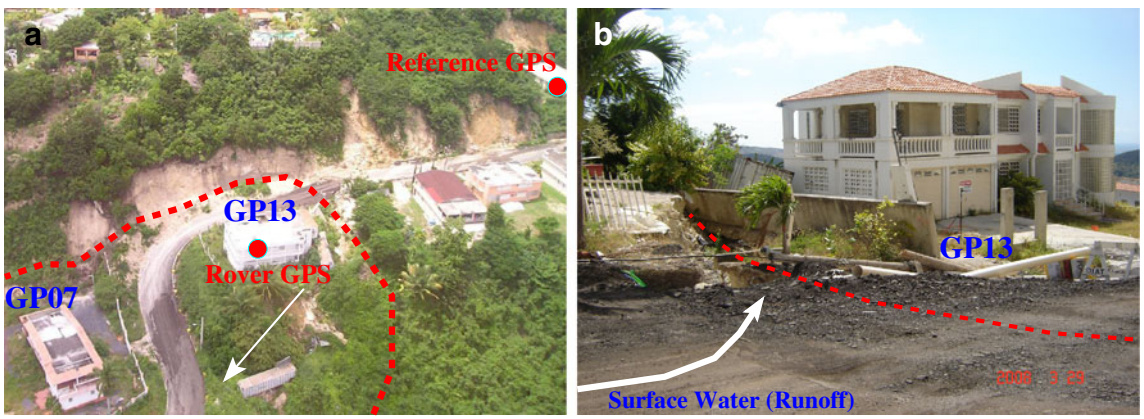

Fig. 9 A close view of the head of the landslide. Benchmarks GP07 and GP13 were installed on the concrete floor in front of each building. A continuous GPS monitoring network, including one rover and one reference GPS stations, has been installed at the head of the landslide since June 1, 2009. The rover GPS was installed on the roof of the two-story building at GP13. The reference GPS (RB in Fig. 1) was installed on the roof of a one-story building outside of the sliding mass

Fig. 10 The continuous GPS station on the two story building at the head of the landslide. The GPS station was equipped with a Trimble NetRS GPS receiver and a choke ring antenna. The GPS receiver was powered by a battery charged by solar power

indicate a linear relationship between the landslide displacement and time during the first 2 months of the continuous monitoring. For this reason, the daily positions during the first 2 months were used to study the repeatability (precision) of the GPS measurements by removing a linear trend. The root mean square (RMS) of the detrended daily position time series was used as an index to evaluate the precision of the GPS measurements. The RMSs of the two horizontal components were 0.5 mm, and the RMS of the vertical component was 1.3 mm.

The right-hand column of Fig. 11 shows the details of the rapid sliding shaded in the left-hand column. It shows a strong correlation between the rainfall and the temporarily rapid sliding. There was continuous moderate rainfall from October 30 to November 12, 2009. The total rainfall during these 2 weeks was about 25 cm. The total landslide displacement was about 0.8 cm in both the NS and EW directions during the rainfall period. There were no significant rapid movements in the vertical direction. The creeping began to accelerate on November 2, 3 days after the start of the rainfall. The total rainfall during those 3 days was only about 5 cm. The rainfall began to increase in intensity on November 7 and continued for 4 days. As a result, the creeping of the landslide was further accelerated and generated rapid sliding from November 7 to 14. The creeping movement returned to the previous sliding rate after November 14, 2009, 2 days after the cessation of the rainfall. The detailed movements will be further studied through hourly GPS resolutions in the following section.

Figure 12 shows the horizontal sliding vector of the continuous GPS antenna during the time range of June to December 2009. It shows a steady movement to the southeast (40°). The rapid movement induced by the prolonged moderate rainfall in November 2009 did not affect the sliding direction. The total horizontal displacement was about 6.5 cm (0.9 cm/month), far less than during the same period in 2008. The total displacement in the latter half of 2008 was about 2 m horizontally and 1 m vertically (Fig. 5). The slower movement in 2009 was largely correlated to decreased rainfall during the year. Figure 13 shows the rainfall data recorded by the USGS meteorological station during the years 2008 and 2009. The total rainfall during 2009 was only about 60% of the total rainfall occurring in 2008. Note that the total rainfall recorded by the rain gauge at the landslide site during 2009 (Fig. 11) was slightly larger than that recorded by the USGS weather station. Due to topography effects, rainfall varies greatly across the island. The average annual rainfall on the southern coast of Puerto Rico is close to 100 cm (The Climate Source Inc 2002; Larsen and Webb 2009). The total rainfall in 2009 was about 85 cm, slightly below average.

Hourly resolutions

In order to track the details of the kinematics of the landsliding, the 24-h continuous sessions were split into hourly sessions. The baseline length at each hour was calculated by using the Topcon software. Figure 14 illustrates the three-component baseline lengths derived from hourly resolutions, within a 10-day window. The left-hand column illustrates a comparison of the daily GPS resolutions processed by the GAMIT software and hourly resolutions processed by the Topcon software. The daily average of these hourly resolutions was also plotted. The hour-by-hour variance superimposed on the hourly position time series might comprise certain random errors within GPS observations and post-processing. There was a constant difference between the daily resolution processed by the GAMIT software and the daily average of the hourly resolutions processed by the Topcon software during the entire time range. The difference, less than 1 mm for the two horizontal components and 3 mm for the vertical component, can be caused by systematic errors related to different post-processing software packages, which effect the absolute baseline lengths but not the changes of baseline lengths (displacements). The right-hand column of Fig. 14 illustrates hourly measurements within a 4-day window. It shows a consistent shift in position from day to night. This is particularly clear in the north–south component. It seems that the antenna was shifted to the south about 1 mm in the morning (about local time 8:00 AM) and then shifted back to the north in the evening (about local time 8:00 PM). This periodic shift probably represents the movement of the building due to solar heat gain during the day and heat loss during the night. This phenomenon is known as thermal movement of buildings in the civil engineering community. Thermal movements can cause cracks in buildings (Dickinson and Thornton 2004). This study indicates that GPS can be used as a precise displacement sensor to study thermal movements of buildings.

Figure 15 illustrates the hourly displacement time series during the prolonged moderate rainfall period that occurred in November 2009. The shaded bar marks the initial sliding of the rapid movement induced by the moderate rainfall that occurred from October 30 to November 11, 2009 (Fig. 11). The average creeping rates before and after the rainfall were 0.2 mm/day. The

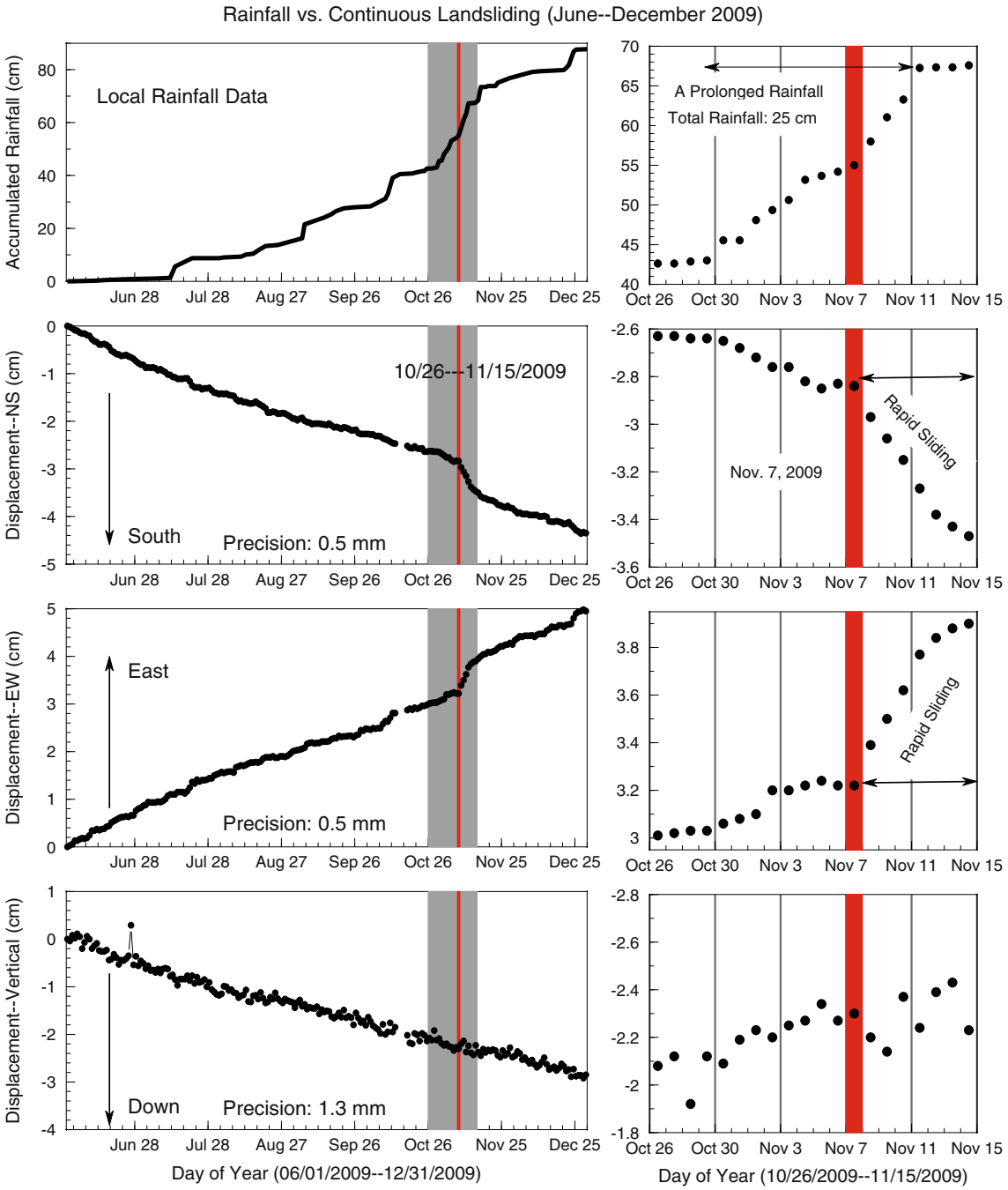

Fig. 11 Three-component daily movements (24-h resolutions) of the landslide derived from continuous landslide monitoring from June to December 2009. The *top row* illustrates rainfall recorded by a rain gauge at the reference GPS site. The daily positions were obtained from single base processing, using the GAMIT GPS software. The baseline length was 130 m. The *right-hand column* shows the details of the rapid slide segment shaded in the *left-hand column*

average rate during the rainfall period was about six times faster (1.2 mm/day). The vertical component did not show considerable rapid movement during the rainfall period, indicating a flat sliding plane. The right-hand column is a 4-day window showing the details of the initial sliding. The NS component indicates a remarkable change in the sliding rate in the morning of November 7 (about GPS time 10:00 AM–12:00 PM; local time 6:00–8:00 AM), indicating the initiation of the rapid sliding. Local precipitation data also show a significant increase in the intensity of the rainfall on the same day (Fig. 11). Unfortunately, the local precipitation data were recorded daily rather than hourly. It is not possible to further identify the latency of the rapid sliding and the amount of total rainfall accumulated before the initial sliding. Landslide responses to rainfall involve transient processes with different intrinsic timescales. The time delay between the initial accelerating of the landslide and the initial rainfall would be a function of rainfall intensity, duration, slope permeability, and slope depth.

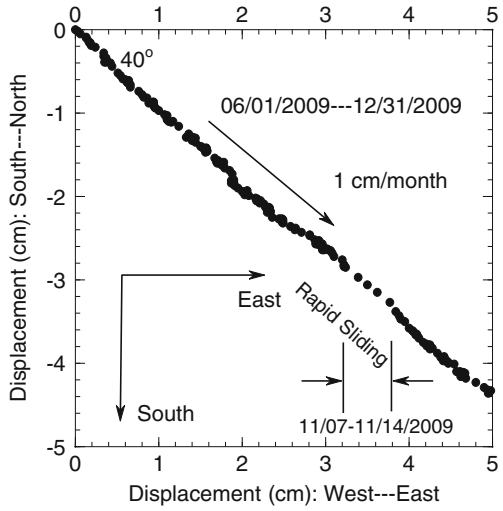

Fig. 12 The horizontal sliding track of the landslide derived from the continuous movements illustrated in Fig. 11. The total horizontal displacement was about 6.5 cm (0.9 cm/month)

Discussion and suggestions

A landslide lawsuit has been filed by local home owners. Determining the causes of the landslide has become a sensitive topic. No single cause can be determined from the existing evidence. A variety of factors may have contributed to the initial failure, including geologic structure, weak clay at the bottom of the colluvium, construction of new houses and swimming pools, cutting at the toe area, use of cesspools, heavy rainfalls, as well as other factors yet to be identified. Rainfall exerted a large influence on the movement of the landslide. Even a moderate rainfall, like the one that occurred in November 2009, could induce a temporary rapid slide. The mechanics of rainfall-induced landsliding are among the most important and difficult issues in landslide study. A number of numerical and observational models about landslide–rainfall relationship have been proposed (Polemio and Sdao 1999; Iverson 2000; Wang and Sassa 2003; Guzzetti et al. 2004). In general, rainfall infiltration into a slope could result in changing soil suction (negative pore pressure) and pore water pressure (positive pore pressure), as well as raising soil unit weight and reducing anti-shear strength of rock and soil (Lan et al. 2003). Increased positive pore pressure has been recognized as the major contributor to the failure of landslides (Terzaghi 1950; Brand 1981; Anderson and Sitar 1995; Wang and Sassa 2003; Matsuura et al. 2008). Unfortunately, groundwater level data and piezometer data were not available for this landslide, inhibiting the study of changes in pore water pressure. For the Cerca del Cielo landslide, sources of increased positive pore pressures might include any or all of the following sources:

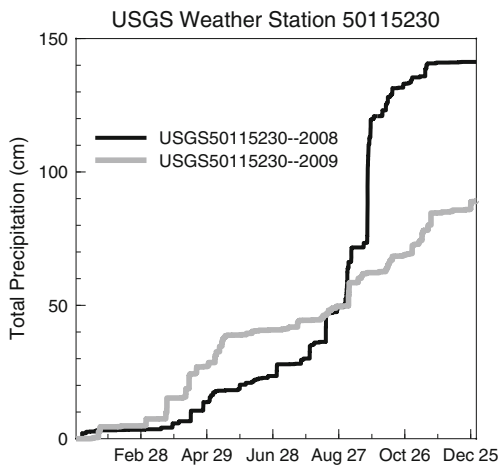

Fig. 13 The accumulated precipitation recorded by the local USGS Weather Station 50115230 (latitude 18°03′07″, Longitude 66°37′41″) during 2008 and 2009

(a) Seepage from domestic sewage

According to site investigations, domestic sewage from this community was directly discharged to cesspools built in back yards or beneath houses. The use of cesspools for sewage is very common in small neighborhoods in Puerto Rico. With the increase in population, more and more domestic sewage was produced and infiltrated into the ground. A number of swimming pools, which were also emptied directly into the ground, had been built in recent years. Both sewage and swimming pool water infiltrated into the inside of the landslide mass, which may have increased pore pressure, thus decreasing the effective stress in the soil and reducing the shear strength of the soil. The domestic sewage problem was also thought to be one of the major contributions to the failure of the 1985 Mameyes, Ponce landslide (Silva-Tulla 1986; Jibson 1986).

(b) Surface water

The community did not have a drainage system. Surface water drained directly onto the surface of the ground and flowed into a stream at the foot of the landslide. There were frequent earthworks at both the head and toe areas in recent years. These human activities may have broken the original continuity of the ground surface and allowed water to flow into the landslide mass, which increased the groundwater level. High groundwater levels may have exerted a negative impact on the stability of the landslide. First, it increased pore water pressure on the sliding surface and reduced the shear strength. Second, it activated the expansion and contraction process of the clay content beneath the colluvium deposits. The clay may have weakened when wet. The situation worsened when cracks and fissures on the ground surface enlarged and allowed more water to flow into the sliding mass. One intensive rainfall in the summer of 2007 may have been what finally triggered the slope failure.

The slide appears likely to continue to move slowly in the future, with short bursts of rainfall-induced temporary rapid movement. The average creeping rate during the latter half of 2009 was about 0.9 cm/month. Continuous observation during early of 2010 indicated that the current average creeping rate was even lower. However, local residents should pay close attention to the sliding during storm seasons and be made aware of significant increases in the sliding rate. The slide can probably not be permanently stabilized economically. The potential damage and risk can, however, be minimized through the following measures:

(a) Improve the surface-drainage system to minimize runoff onto the sliding mass.

Minimizing the infiltration of water into the sliding mass would be critical to minimizing the landslide movement.

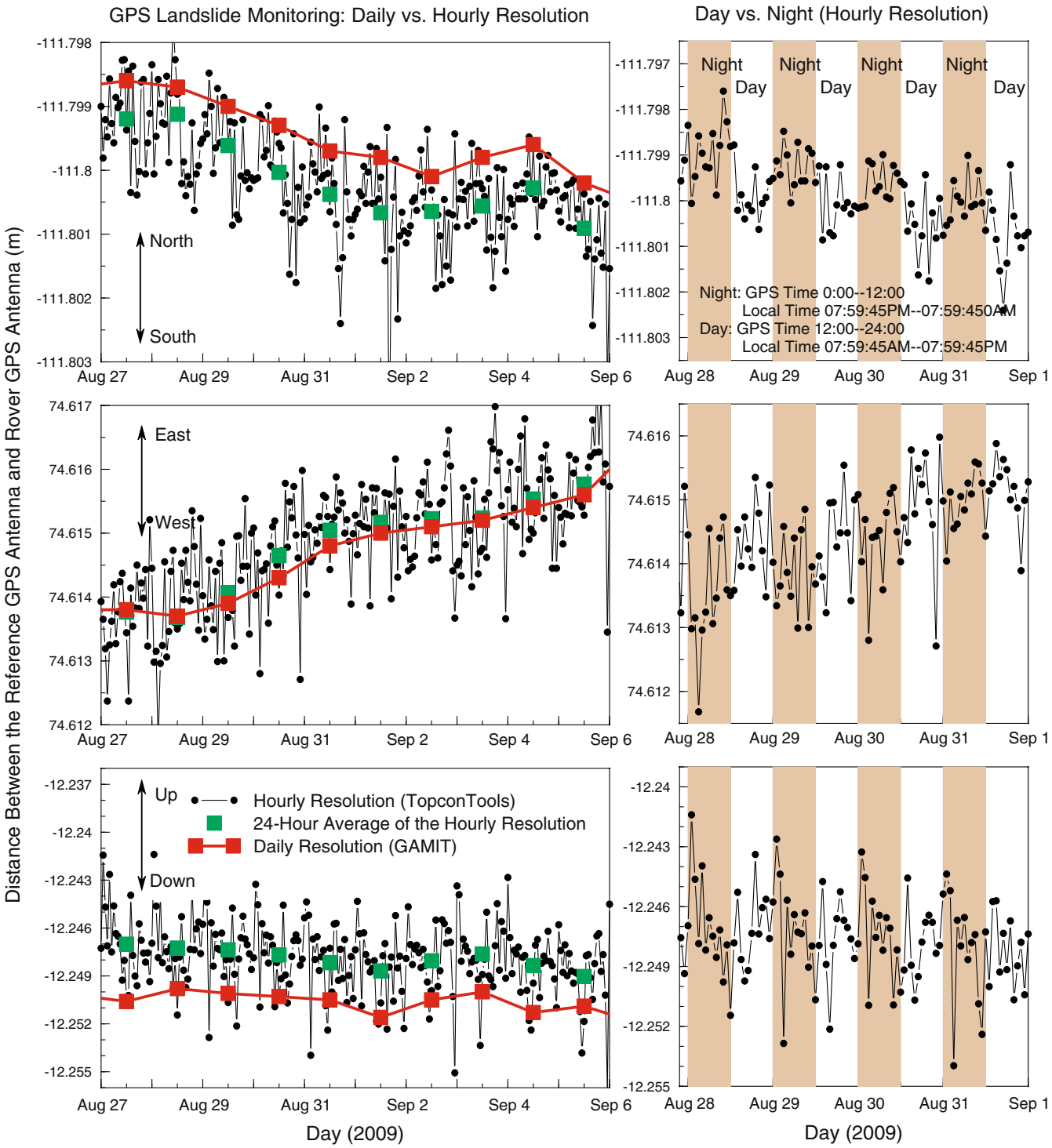

Fig. 14 Thermal movements of the building inferred from hourly GPS resolutions. The Topcon Tools software was applied in hourly data processing. The *Y*-axis represents the baseline length between the landslide and reference GPS stations. The *X*-axis represents the global positioning system time

Currently, the streets both inside and outside the sliding mass have no storm drains, with all the runoff emptying directly into the sliding mass through the head scarp and inside fissures. The area just north of the landslide head is a large open drainage area. All surface water accumulated in this drainage area flows into the landslide mass during rainfall. It would be very advantageous to construct a drainage channel to the north of the landslide head in order to intercept any runoff coming from the highlands outside of the landslide and divert it to the outside of the sliding mass. The drainage system inside the sliding mass area should also be improved.

(b) Conduct real-time GPS monitoring

This landslide remains active and has a potential to develop further during future storm seasons. A large slide could cause

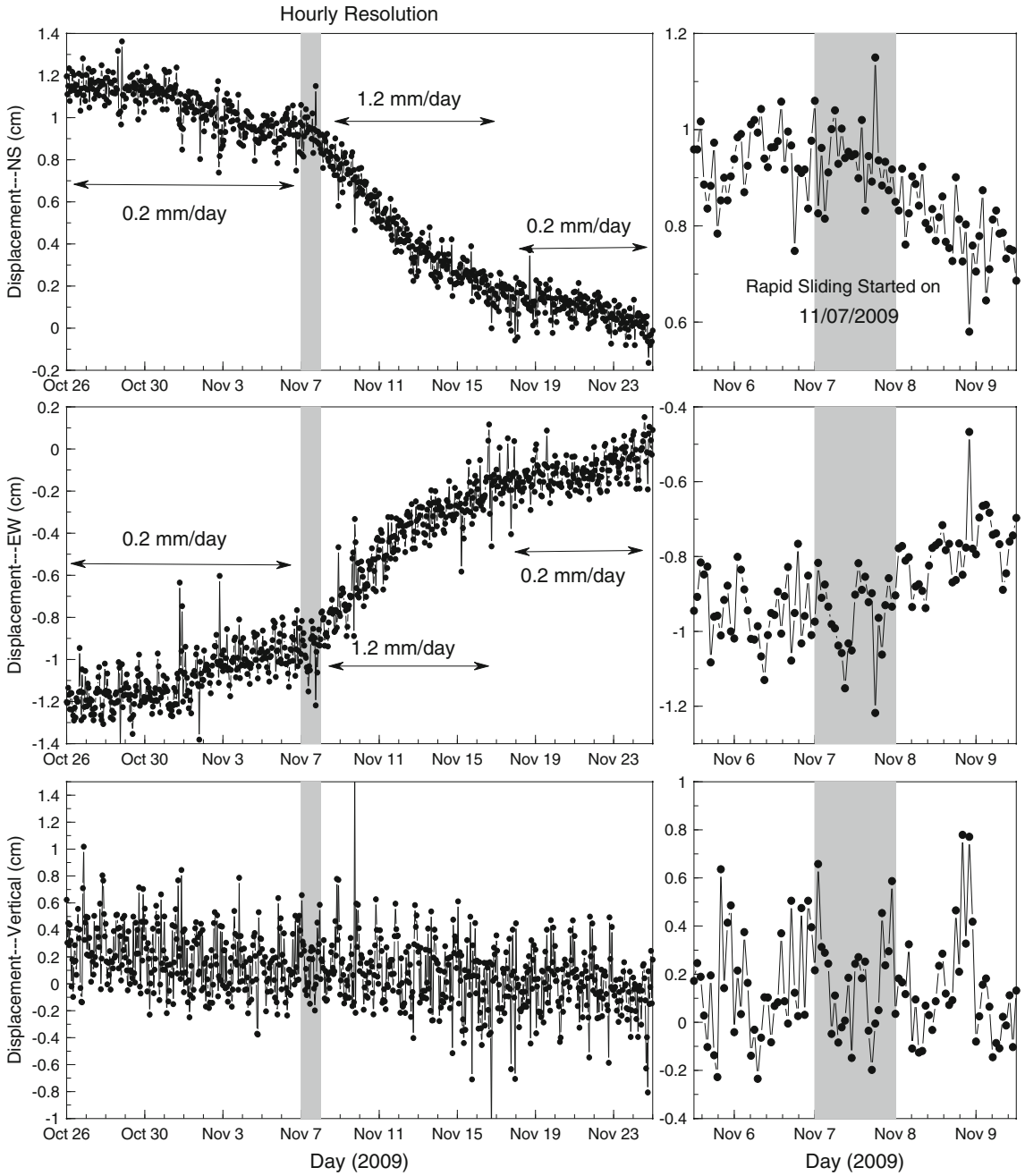

Fig. 15 Hourly displacements of the rapid slide period shaded in Fig. 11. The *right-hand column* highlights the initiation of the rapid sliding, which began on November 7, 2009

further damage, even catastrophic collapse of buildings along the sole access road. The two-story buildings at the head zone would be particularly imperiled and could threaten the safety of the people driving across the sliding mass (see Fig. 9). It is possible that the whole sliding mass could slide to the lower area during a prolonged heavy rainfall. This would completely cut transportation routes, as well as the water and power supply of the entire community. There are still about 50 families residing in the community. It would be useful to conduct real-time GPS monitoring at the landslide site. Real-time monitoring can detect early indications of rapid movement. Significant increases in the rate of movement could be quickly reported to the local government and inhabitants for their safety.

Acknowledgments

I acknowledge Dr. James Joyce (University of Puerto Rico at Mayaguez) for many thoughtful discussions about the geology aspects of this landslide and Mr. Cesar E. Pujos (Department of Transportation, Puerto Rico) for supplying local maps and geotechnical documents. I appreciate Dr. Robert W. King (MIT) for answering many questions related to the GAMIT software and

his comments on an early version of this manuscript. I would also like to acknowledge Mr. Carlos Ponce for his support in our research and education activities at the landslide site. Many undergraduate students in the Departments of Geology and Civil Engineering at the University of Puerto Rico-Mayaguez have been involved in the field surveying. I appreciate their hard work. This study was funded by NSF projects (EAR-0722540, EAR-0842314) and a NASA Puerto Rico Space Grant. The two continuous GPS units were provided by UNAVCO through its Equipment Loan Program. I appreciate Jim Normandeau, Frederick Blume, and Charles Meertens (UNAVCO) for their technical support.

References

Anderson SA, Sitar N (1995) Analysis of rainfall-induced debris flow. J Geotech Eng ASCE 121(7):544–552

Avila LA (2008) Tropical cyclone report—Hurricane Kyle. National Hurricane Center. : http://www.nhc.noaa.gov/pdf/TCR-AL112008_Kyle.pdf. Accessed 29 Nov 2009

Banuchi R (2008) Heavy rains drench Puerto Rico. USA Today (September 23, 2008). http://www.usatoday.com/weather/storms/2008-09-22-puerto-rico-flooding-rains_N.htm. Accessed 29 Nov 2009

Baum RL, Chleborad AF, Schuster RL (1998) Landslides triggered by the December 1996 and January 1997 storms in the Puget Sound area, Washington. US Geological Survey Open-File Report 98-239

Brand EW (1981) Some thoughts on rainfall induced slope failures. Proceedings of 10th International Conference on Soil Mechanics and Foundation Engineering, pp 373–376

Bruckl E, Brunner FK, Kraus K (2006) Kinematics of a deep-seated landslide derived from photogrammetric, GPS and geophysical data. Eng Geol 88:149–159

Coe JA, Ellis WL, Godt JW, Savage WZ, Savage JE, Michael JA, Kibler JD, Powers PS, Lidke DJ, Debray S (2003) Seasonal movement of the Slumgullion landslide determined from global positioning system surveys and field instrumentation, July 1998–March 2002. Eng Geol 68:67–101

Dickinson PR, Thornton N (2004) Cracking and building movement, published by RICS Business Services Limited, ISBN 1-84219-156-x. The Royal Institute of Chartered Surveyors, UK

Dogan U (2007) Accuracy analysis of relative positions of permanent GPS stations in the Marmara region, Turkey. Surv Rev 39(304):156–165

Eckl MC, Snay RA, Soler T, Cline MW, Mader GL (2001) Accuracy of GPS derived relative positions as a function of interstation distance and observing-session duration. Journal of Geodesy 75:633–640

Frei E, Beutler G (1990) Rapid static positioning based on the fast ambiguity resolution approach (FARA): theory and first results. Manuscripts Geodaetia 15:325–356

Gili JA, Corominas J, Rius J (2000) Using global positioning system techniques in landslide monitoring. Eng Geol 55:167–192

Guzzetti F, Cardinali M, Reichenbach P, Clipolla F, Sebastiani C, Galli M, Salvati P (2004) Landslides triggered by the 23 November 2000 rainfall event in the Imperia Province, Western Liguria, Italy. Eng Geol 73:229–245

Guzzetti F, Peruccacci S, Rossi M, Stark CP (2008) The rainfall intensity–duration control of shallow landslides and debris flows: an update. Landslides 5:3–17

Herring TA, King RW, McCluskey SM (2009) Introduction to GAMIT/GLOBK, release 10.35. MIT, Cambridge

Iverson RM (2000) Landslide triggering by rain infiltration. Water Resour Res 36 (7):1897–1910

Jibson RW (1986) Evaluation of landslide hazards resulting from the 5–8 October 1985 storm in Puerto Rico. U.S. Geological Survey Open-File Report 86-26

Jibson RW (1989) Debris flows in southern Puerto Rico. Geol Soc Am, special paper 236, pp 29–55

Joyce J (2008) Geology of the Cerca del Cielo landslide site. Geotechnical report on landslide investigation, analyses and remedial measures at Cerca Del Cielo Community Tallaboa Ward, Ponce, Puerto Rico. Suelos Inc., May 2008 (Engineering report, not formally published)

Krushensky RD, Monroe WH (1978) Geological map of the Penuelas and Punta Cuchara quadrangles, Puerto Rico: U.S. Geological Survey miscellaneous investigations map I-1042, scale 1:20,000

Lan H, Zhou C, Lee CF, Wang S, Wu F (2003) Rainfall-induced landslide stability analysis in response to transient pore pressure. Science in China Ser E Technological Sciences 46:52–68

Larsen MC (2008) Rainfall-triggered landslides, anthropogenic hazards, and mitigation strategies. Advances in Geosciences 14:147–153

Larsen MC, Simon A (1993) Rainfall-threshold conditions for landslides in a humid-tropical system, Puerto Rico. Geografiska Annaler 75A(1–2):13–23

Larsen MC, Torres-Sanchez AJ (1996) Geographic relations of landslide distribution and assessment of landslide hazards in the Blanco, Cibuco, and Coamo river basins, Puerto Rico. U.S. Geological Survey Water-Resources Investigations Report 95-4029, 56 p

Larsen MC, Torres-Sanchez AJ (1998) The frequency and distribution of recent landslides in three Montane tropical regions of Puerto Rico. Geomorphol 24(4):309–331

Larsen MC, Webb RMT (2009) Potential effects of runoff, fluvial sediment, and nutrient discharges on the Coral Reefs of Puerto Rico. J of Coast Res 25:189–208

Larsen MC, Santiago M, Jibson R, Questell E (2004) Map showing susceptibility to rainfall-triggered landslides in the municipality of Ponce, Puerto Rico. U.S. Geological Survey Scientific Investigations Map I-2818, 1 p

Malet JP, Maquaire O, Calais E (2002) The use of global positioning system techniques for the continuous monitoring of landslides—application to the Super-Sauze earthflow (Alpesde Haute-Province, France). Geomorphol 43:33–54

Matsuura S, Asano S, Okamoto T (2008) Relationship between rain and/or meltwater, pore-water pressure and displacement of a reactivated landslide. Engineering Geology 101:49–59

Monroe WH (1964) Large retrogressive landslides in north-central Puerto Rico. U.S. Geological Survey Professional Paper 501, Chapter B, B123–B125

Monroe WH (1979) Map showing landslides and areas of susceptibility to landsliding in Puerto Rico. U.S. Geological Survey Miscellaneous Investigations Series Map I-1148, 1 sheet, scale 1:240,000

Mora P, Baldi P, Casula G, Fabris M, Ghirotti M, Mazzini E, Pesci A (2003) Global positioning systems and digital photogrammetry for the monitoring of mass movements: application to the Ca di Malta landslide (northern Apennines, Italy). Eng Geol 68:103–121

Peyret M, Djamour Y, Rizza M, Ritz JF, Hurtrez JE, Goudarzi MA, Nankali H, Chery J, Le Dortz K, Uri F (2008) Monitoring of the large slow Kahrod landslide in Alboz mountain range (Iran) by GPS and SAR interferometry. Eng Geol 100:131–141

Polemio M, Sdao F (1999) The role of rainfall in the landslide hazard: the case of the Avigliano urban area (Southern Apennines, Italy). Eng Geol 53:297–309

Psimoulis P, Ghilardi M, Fouache E, Stiros S (2007) Subsidence and evolution of the Thessaloniki plain, Greece, based on historical leveling and GPS data. Eng Geol 90:55–70

Sato HP, Abe K, Ootaki O (2003) GPS-measured land subsidence in Ojiya City, Niigata Prefecture, Japan. Eng Geol 67:379–390

Silva-Tulla F (1986) The October 1985 landslide at Barrio Mameyes, Ponce. National Academy, Washington, D.C

Soler T, Michalak P, Weston ND, Snay RA, Foote RH (2006) Accuracy of OPUS solutions for 1- to 4-h observing sessions. GPS Solut 10(1):45–55. doi:10.1007/s10291-005-0007-3

Squarzoni C, Delacourt C, Allemand P (2005) Differential single-frequency GPS monitoring of the La Valette landslide (French Alps). Eng Geol 79:215–229

Suelos Inc. (2008) Geotechnical report on landslide investigation, analyses and remedial measures at Cerca Del Cielo Community Tallaboa Ward, Ponce, Puerto Rico (engineering report)

Tagliavini F, Mantovani M, Marcato G, Pasuto A, Silvano S (2007) Validation of landslide hazard assessment by means of GPS monitoring technique—a case study in the Dolomites (Eastern Alps, Italy). Nat Hazards and Earth System Sciences 7:185–193

Terzaghi k (1950) Mechanism of landslides. In: Paige S (ed) Application of geology to engineering practice. Geological Society of America, New York, pp 83–123

The Climate Source Inc. (2002) PRISM 1963–1995 mean annual precipitation, Puerto Rico. http://www.climatesource.com/pr/fact_sheets/prppt_xl.jpg. Accessed 05 Jan 2010

Wang G, Sassa K (2003) Pore-pressure generation and movement of rain-fall-induced landslides: effects of grain size and fine-particle content. Eng Geol 69:109–125

Wang G, Phillips D, Joyce J, Rivera FO (2011) The integration of TLS and continuous GPS to study landslide deformation: a case study in Puerto Rico. J of Geodetic Sci 1 (1):25–34. doi:10.2478/v10156-010-0004-5

G.-Q. Wang (✉)
Puerto Rico Seismic Network, Department of Geology,
University of Puerto Rico at Mayaguez,
P.O. Box 9000, Mayaguez, PR, USA
e-mail: guoquan.wang@upr.edu